





<b>Publication Year</b>	2013
<b>Acceptance in OA</b>	2023-02-21T07:23:02Z
<b>Title</b>	LAD Background variation and systematics
<b>Authors</b>	DEL MONTE, Ettore, CAMPANA, RICCARDO, FEROCI, MARCO, DE ROSA, Alessandra, Fraser, George, Nowak, Michael, ORLANDINI, MAURO, Perinati, Emanuele, Uttley, Phil, Vaughan, Simon, Walton, Dave
<b>Handle</b>	<a href="http://hdl.handle.net/20.500.12386/33645">http://hdl.handle.net/20.500.12386/33645</a>
<b>Volume</b>	LOFT-LAD-BkgSys-20130918

	<p style="text-align: center;">LOFT</p> <p style="text-align: center;">LAD</p>	<p><b>Doc. no. :</b> LOFT-LAD-BkgSys-20130918  <b>Issue :</b> 1.0  <b>Date :</b> 18 September 2013  <b>Cat :</b>  <b>Page :</b> 1 of 23</p>
---	--	---


**LOFT Large Area Detector**  
**LAD Background variation and systematics**

	Name	Date	Signature
Prepared by	R. Campana E. Del Monte M. Feroci, A. De Rosa, G. Fraser, M. Nowak, M. Orlandini, E. Perinati, P. Uttley, S. Vaughan, D. Walton (the Background Working Group)	2013-09-18	
Verified by			
Authorized by			

	<p style="text-align: center;">LOFT</p> <p style="text-align: center;">LAD</p>	<p><b>Doc. no. :</b> LOFT-LAD-BkgSys-20130918  <b>Issue :</b> 1.0  <b>Date :</b> 18 September 2013  <b>Cat :</b>  <b>Page :</b> 2 of 23</p>
---	--	---


### Document Change Record

Issue	Date	Changed Section	Description of Change
1	2013-09-18	All	First issue

	<p>LOFT</p> <p>LAD</p>	<p><b>Doc. no. :</b> LOFT-LAD-BkgSys-20130918  <b>Issue :</b> 1.0  <b>Date :</b> 18 September 2013  <b>Cat :</b>  <b>Page :</b> 3 of 23</p>
---	------------------------	---

## Table of contents

<b>1</b>	<b>Introduction .....</b>	<b>4</b>
<b>2</b>	<b>Overview of the LAD background .....</b>	<b>5</b>
<b>3</b>	<b>Background modulation .....</b>	<b>6</b>
<b>4</b>	<b>Other background variability sources .....</b>	<b>10</b>
4.1	Strong off-axis sources .....	10
4.2	Solar activity .....	14
4.3	The Galactic Ridge X-ray Emission (GRXE).....	15
<b>5</b>	<b>Blank field monitoring .....</b>	<b>15</b>
<b>6</b>	<b>Active monitoring .....</b>	<b>17</b>
<b>7</b>	<b>Conclusions .....</b>	<b>18</b>
<b>8</b>	<b>Appendix 1 - Context: The RXTE/PCA background modelling .....</b>	<b>20</b>
<b>9</b>	<b>References .....</b>	<b>23</b>

	<p style="text-align: center;">LOFT</p> <p style="text-align: center;">LAD</p>	<p><b>Doc. no. :</b> LOFT-LAD-BkgSys-20130918  <b>Issue :</b> 1.0  <b>Date :</b> 18 September 2013  <b>Cat :</b>  <b>Page :</b> 4 of 23</p>
---	--	---

## 1 Introduction

The study of the properties of matter accreting in a Strong Gravity field is among the scientific objectives of the LOFT mission. Two different and independent methods can be employed for this type of investigations: timing measurements of Quasi Periodic Oscillations, which occur at the dynamical time scale of the innermost disk regions and hence are associated to the fundamental frequencies of matter motion in strong field gravity, and spectral measurements of the Fe  $K\alpha$  lines, emitted in many accreting collapsed objects, from neutron stars to supermassive black holes in AGNs.

In particular, the relativistically broadened Fe-line profile that is seen in a number of AGNs (with a flux of a few mCrab) provides a powerful tool to probe the accretion flow in a region where the motion is determined by General Relativity. In addition, the measure of the emitting radius can be derived from the investigation of the line response to flares and the “reverberation” of the central source features in the line profile. These spectral studies particularly benefit from the high energy resolution, wide energy band and high sensitivity of the LOFT Large Area Detector (LAD). Since the LAD is a collimated and non-imaging instrument, the background cannot be simultaneously measured, and then subtracted, during the source observation (as it usually happens in imaging instruments) but it has to be carefully “a priori” modelled and calibrated.

Preliminary evaluations already indicated that the uncertainty on the knowledge of the LAD background has to be reduced below a few percent in order to efficiently exploit the performance of the instrument in the Strong Gravity studies. In fact, the average background level will be subtracted from the signal, but its fluctuations, if not properly modelled, may affect the observation of faint sources. Given the huge throughput of the LAD and the high statistics that can be accumulated even with short integrations, particular care must be taken in the evaluation and reduction of all the systematic effects, that will ultimately affect the instrument capabilities in this type of studies. The systematic effects derive from the *unmodelled* and *uncorrected* variations of the background, that are consequently not properly subtracted from the signal of faint sources. Therefore specific activities have been devoted to address a full characterisation of the LAD background variability and define models to describe it and to estimate the resulting accuracy of the subtraction.

The structure of this document is as follows. The instrument mass model and background components used in the simulation of the LAD background spectrum are briefly summarised in Section 2. Section 3 describes the orbital background modulation that arises from the different attitude of the satellite with respect to the background sources. Section 4 deals with two other sources of background variability, namely strong off-axis sources and solar flaring activity. The modelling of the background variability using the observation of blank fields, and the evaluation of the accuracy that can be reached, and consequently on the residual systematic effects, is discussed in Section 5. In Section 6 we discuss the possibility to employ an active monitoring of the background. Finally, in Section 7 we draw our conclusions. The issues of the background calibration of a large area collimated instrument for timing that have been tackled in the case of the Proportional Counter Array (PCA; [RD2]) onboard the RXTE mission, although in a different instrumental context, will be described in Appendix 1.

	<p>LOFT</p> <p>LAD</p>	<p><b>Doc. no. :</b> LOFT-LAD-BkgSys-20130918</p> <p><b>Issue :</b> 1.0</p> <p><b>Date :</b> 18 September 2013</p> <p><b>Cat :</b></p> <p><b>Page :</b> 5 of 23</p>
---	------------------------	---

## 2 Overview of the LAD background

The LOFT/LAD background has been simulated using a GEANT-4 Monte Carlo mass model, and the results are discussed in [RD1].

The main background contribution is due to the high energy photons leaking from the MCP collimator and coming from the cosmic diffuse X-ray background (CXB) and the Earth albedo emission. Other background components are due to internal radioactivity and particles (protons, neutrons, electrons and positrons from primary cosmic rays and Earth atmosphere), and from the diffuse radiation collected in the field of view (aperture background). Activation-induced background is found to be negligible, due to the low mass of the instrument and its favourable low-altitude, low-inclination orbit<sup>1</sup>. The average background components and their contributions to the resulting fluxes are shown in Figure 1, while Figure 2 shows the weight of the various components.

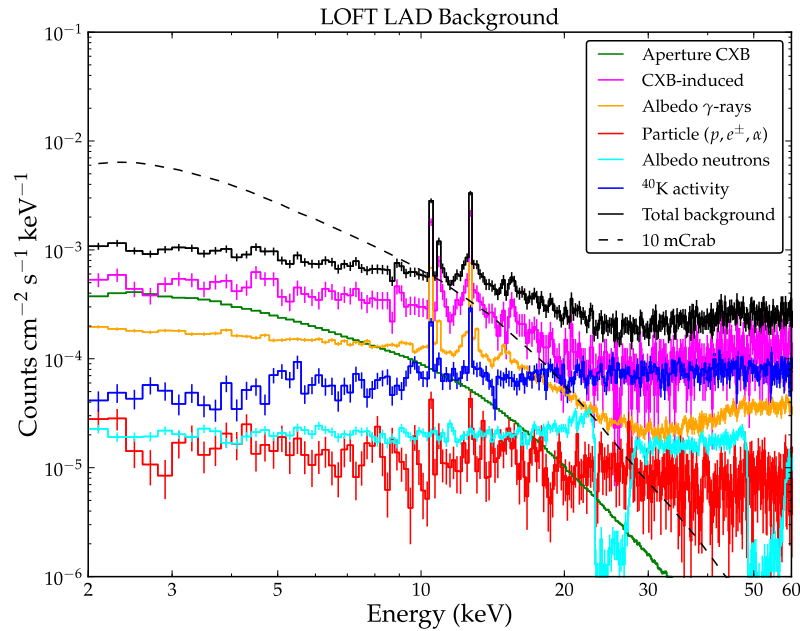


Figure 1 - The LOFT/LAD background

<sup>1</sup> We simulated the activation of the LAD materials inside the SAA with GEANT adopting a simplified mass model, including only the collimator and the SDD. We represent the input proton spectrum in the SAA with a power-law of -3 index, normalised to the flux ( $\sim 2 \text{ p/cm}^2/\text{s}$ ) estimated with the SPENVIS package for the LOFT nominal orbit and adopted for the radiation damage studies. Assuming that the passage in SAA has an average duration of 700 s, we obtain  $\sim 2 \times 10^{-5} \text{ cts/cm}^2/\text{s}$  (corresponding to 3 cts/s for the whole LAD surface and 0.09% of the overall background) in the energy band 2–30 keV and in a time window between 1 min and 90 min after the egress from the SAA, that is during the remainder of the orbit before the next passage. This contribution includes both the prompt and delayed components, up to 90 min after the SAA passage.

	<p style="text-align: center;">LOFT  LAD</p>	<p><b>Doc. no. :</b> LOFT-LAD-BkgSys-20130918  <b>Issue :</b> 1.0  <b>Date :</b> 18 September 2013  <b>Cat :</b>  <b>Page :</b> 6 of 23</p>
---	--	---

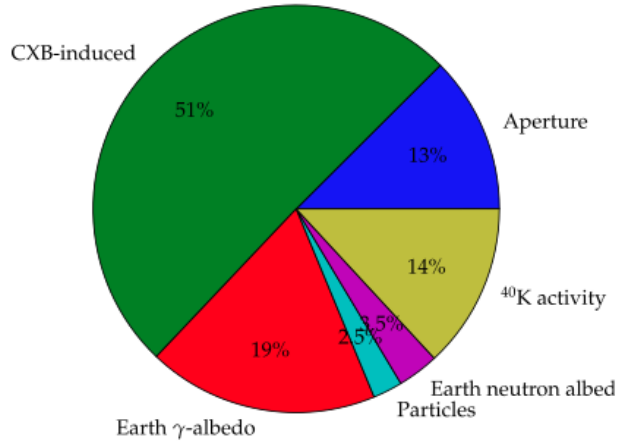


Figure 2 - The weight of the various contributions to the overall background.

The CXB and Earth albedo, the dominant background contributions, are steady sources, while the particle components vary of a few tens of a percent on solar-cycle timescales ( $\sim 11$  years). Another steady background source is due to the radioactive decay of the isotope  $^{40}\text{K}$  contained in the lead glass of the microcapillary plate collimator, that has the very long half-life of  $1.3 \times 10^9$  years.

Although the background sources have a flux intrinsically steady and predictable, a varying relative orientation of the LAD in its radiation environment (i.e. different viewing geometry along the orbit and satellite attitudes) will cause a small and smooth modulation of the detected background due to their different intensity and spectra, on the orbital timescales ( $\sim 90$  min). As we will show in the following Section 3, this effect has been studied through simulations, finding that the maximum expected modulation of the background is less than 10%.


This value has to be compared to a factor of a few for instruments dominated by particle-induced background. For example, RXTE/PCA had up to a  $\sim 250\%$  variation on orbital timescales [RD2]. In the LOFT case, the effect of the other potentially varying sources, i.e. particle induced background, is greatly reduced by the very stable environment offered by the low Earth equatorial orbit. Moreover, as discussed in [RD1], the particle background is further suppressed by the signature that it leaves on the SDD detector (multi-anode events) and its typical energy scale is higher than the 2-80 keV LAD energy band. As a result, this component accounts for less than 6% of the overall background.

Another source of background variability, that also can easily modelled, is due to the contribution of strong off-axis point-like sources (Section 4)

Moreover, we will show the results of the residual level of systematics in the determination of the background that can be reached using the modelling based on the observation of blank fields, and using an "active" monitoring strategy (Section 5 and 6).

### 3 Background modulation

In this discussion, we will use the following reference system. We define  $\theta_E$  as the polar angle between the LAD pointing direction (boresight) and the center of the Earth (Figure

	<p>LOFT</p> <p>LAD</p>	<p><b>Doc. no. :</b> LOFT-LAD-BkgSys-20130918</p> <p><b>Issue :</b> 1.0</p> <p><b>Date :</b> 18 September 2013</p> <p><b>Cat :</b></p> <p><b>Page :</b> 7 of 23</p>
---	------------------------	---

3).

Therefore,  $\theta_E=0^\circ$  represents the Earth center aligned with the field of view, while  $\theta_E=180^\circ$  stands for the Earth at the instrument nadir.

At the LOFT orbital altitude of 550-600 km, the Earth subtends an angle of about  $66^\circ$  around  $\theta_E$ , that translates in a blocking factor of about 30% of the whole sky.

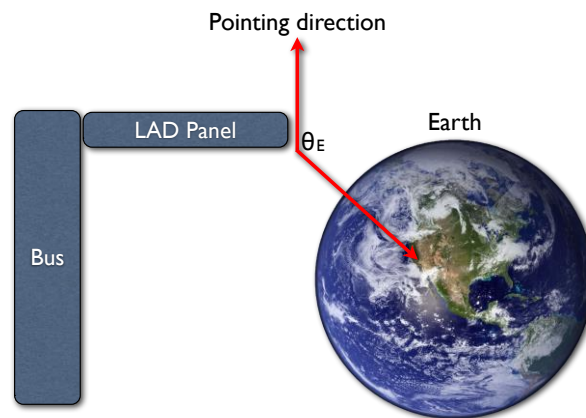


Figure 3 - The viewing geometry

The fluxes of the various background components in the 2-30 keV band, as a function of  $\theta_E$  and thus of the location of the Earth in the LAD reference frame, are shown in Figure 4.

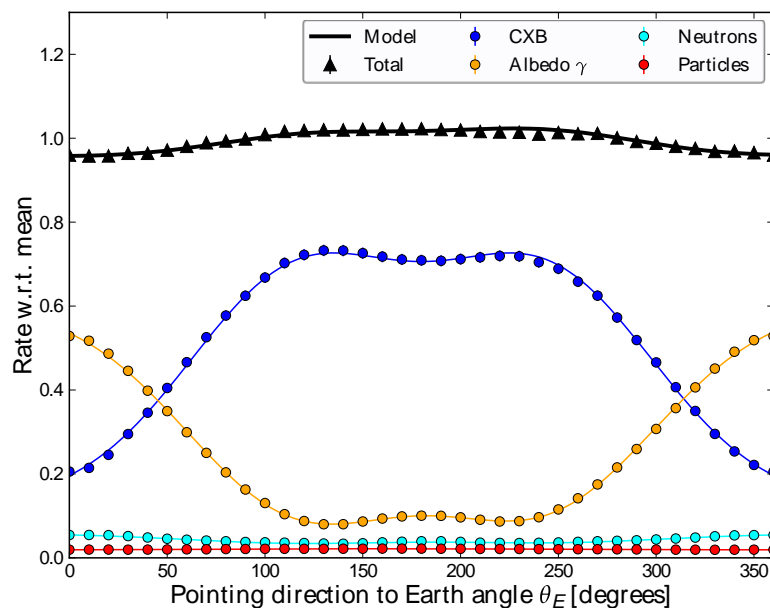


Figure 4 - The background modulation as a function of the Earth location with respect to the pointing direction



	<p style="text-align: center;">LOFT</p> <p style="text-align: center;">LAD</p>	<p><b>Doc. no. :</b> LOFT-LAD-BkgSys-20130918  <b>Issue :</b> 1.0  <b>Date :</b> 18 September 2013  <b>Cat :</b>  <b>Page :</b> 8 of 23</p>
---	--	---

The curve representing the total background (black symbols) shows a maximum modulation of  $\sim 8\%$ .

As discussed above, the modulation of the background rate is due to geometrical effects and it can be predicted and modeled. Each background component is well represented as a function of the Earth location with respect to the pointing direction ( $\theta_E$ ) by a model consisting of two Gaussian distributions, centered at about  $\theta_E = 0^\circ$  and  $180^\circ$ , and a continuum constant level. These distributions, also reported in Figure 4, arise from the convolution of the directional “transparency” of the LAD instrument with the Earth-occulted field of view.

When the detector points towards the zenith ( $\theta_E = 180^\circ$ ) the contribution from the leaking CXB emission is maximum. On the contrary, it is minimum during the maximal Earth occultation ( $\theta_E = 0^\circ$ ), where the Earth albedo contribution reaches its maximum. The overall convolution of these out-of-phase components results in a very small fluctuation of the total background.

For an actual pointing towards an astrophysical source, the range of possible Earth angles  $\theta_E$  is restricted, from a fixed value  $\theta_E = 90^\circ$  for a source at the orbital pole (that is nearly coincident with the Celestial pole, due to the low orbital inclination of LOFT) to the full  $0^\circ$ - $180^\circ$  range for near-equatorial sources.

The fact that the astrophysical sources in the LOFT observing plan are distributed in declination lowers the background modulation further below the maximum during the observation of a realistic scientific target, as shown in Figure 5.

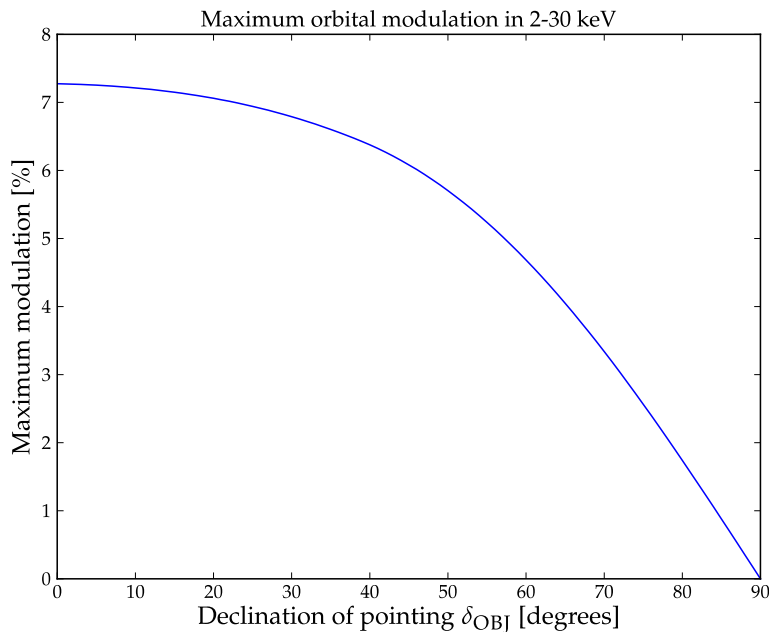


Figure 5 - Maximum orbital modulation of the background flux as a function of the (absolute) value of the celestial declination of the pointing target.

From the knowledge of the background rate vs.  $\theta_E$ , i.e. our background model, it is possible to derive the expected value of the background during the observation of an astrophysical target, as a function of the orbital location and source declination.

For example, Figure 6 shows the values of  $\theta_E$  along a LOFT orbit where the LAD is pointing

	<p style="text-align: center;">LOFT</p> <p style="text-align: center;">LAD</p>	<p><b>Doc. no. :</b> LOFT-LAD-BkgSys-20130918</p> <p><b>Issue :</b> 1.0</p> <p><b>Date :</b> 18 September 2013</p> <p><b>Cat :</b></p> <p><b>Page :</b> 9 of 23</p>
---	--	---

a target at  $\delta = 30^\circ$ . The dashed line indicates the Earth occultation, i.e. for orbital locations in which  $\theta_E$  is below this line the target is Earth-occulted.

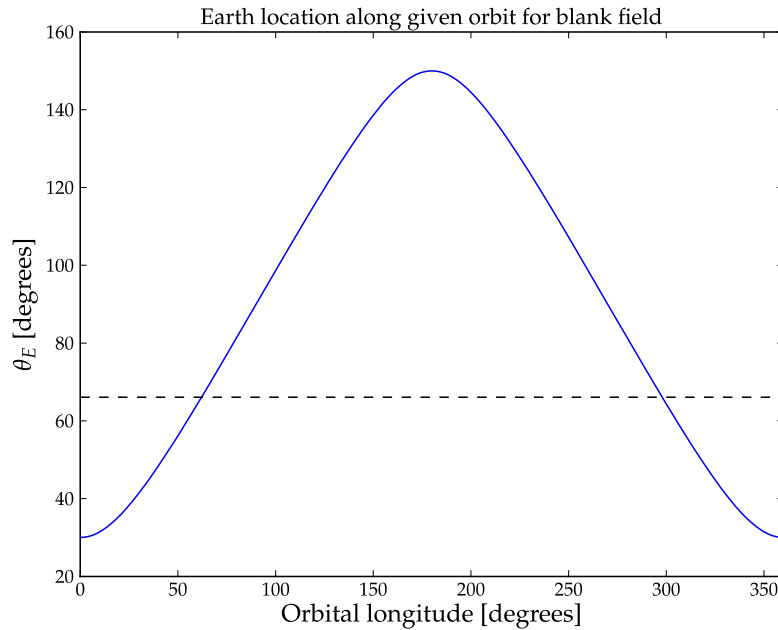


Figure 6 - Angle  $\theta_E$  as a function of the orbital location, for a pointing a source having celestial declination  $\delta = 30^\circ$ . The dashed line indicates the Earth size, i.e., all points below the line are Earth-occulted.

Moreover, in Figure 7 we show the expected background modulation along this orbit, as derived from the geometrical model. The discontinuous jump is due to the Earth occultation, that effectively removes the aperture background.

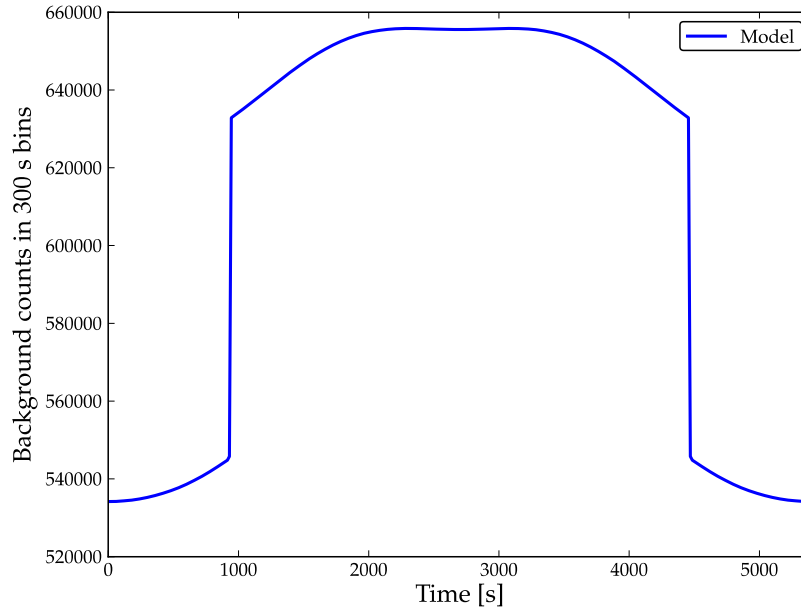


Figure 7 - Background modulation for an orbit where the pointing is at  $\delta = 30^\circ$ . Outside the occultation, the modulation is  $\sim 7\%$  of the average value.

## 4 Other background variability sources

### 4.1 Strong off-axis sources

To evaluate which are the point-like sources whose flux can leak through the collimator and can affect the LAD background, we extracted from the Swift/BAT hard X-ray survey page<sup>2</sup> a list of sources having peak flux above 500 mCrab in 15-50 keV (see Table 1) for more than 1% of the time. For these sources we computed the flux in two energy bands, 15-50 keV and 50-150 keV, using the Swift/BAT data and the spectral models adopted in the compilation of the catalogue by [RD4]. In the same table we also list the hardness ratio as the ratio of the counting rate in 30–150 keV to the rate in 14–150 keV and we include the fraction of time spent by each source above a flux of 500 mCrab. Adopting the criterion of peak flux above 500 mCrab for more than 1% of the time, the sample is composed of 10 objects and includes 7 *persistent* sources and 3 *transient* ones. With the exception of Sco X-1, all the sources in the sample are within  $6^\circ$  from the Galactic Plane. The colour code in the table indicates the expected amount of background increase from each object.

<sup>2</sup> <http://swift.gsfc.nasa.gov/docs/swift/results/transients/>


	<h1 style="text-align: center;">LOFT LAD</h1>	<b>Doc. no. :</b> LOFT-LAD-BkgSys-20130918 <b>Issue :</b> 1.0 <b>Date :</b> 18 September 2013 <b>Cat :</b> <b>Page :</b> 11 of 23
---	---	---

Table 1 - Characteristics of the sample of sources which spend more than 1% of the time above 500 mCrab in 15-50 keV. The Swift/BAT fluxes in two energy bands (15-50 keV and 50-150 keV) are derived from the fit of the Palermo catalogue (<http://www.ifc.inaf.it/cgi-bin/bat/main/fonti.cgi?cat=1>). The time spent by each object above 500 mCrab is computed in the 15-50 keV band. The colours indicate the expected amount of background increase (**red** = important; **orange** = small; **green** = negligible).

Source	l [deg]	b [deg]	Flux <sub>15-50</sub> [mCrab]	Flux <sub>50-150</sub> [mCrab]	Time > 500 mCrab	Hardness Ratio
Persistent sources			Average fluxes	Average fluxes	15-50 keV	
<b>Crab</b>	<b>184.56</b>	<b>-5.78</b>	<b>1000</b>	<b>1000</b>	<b>100%</b>	<b>0.369</b>
<b>Vela X-1</b>	<b>263.06</b>	<b>+3.93</b>	<b>249</b>	<b>18</b>	<b>10%</b>	<b>0.145</b>
<b>GX 301-2</b>	<b>300.10</b>	<b>-0.04</b>	<b>178</b>	<b>2</b>	<b>12%</b>	<b>0.068</b>
<b>Sco X-1</b>	<b>359.09</b>	<b>+23.78</b>	<b>1100</b>	<b>11</b>	<b>100%</b>	<b>0.098</b>
<b>4U 1700-377</b>	<b>347.75</b>	<b>+2.17</b>	<b>189</b>	<b>63</b>	<b>2%</b>	<b>0.252</b>
<b>GRS 1915+105</b>	<b>45.37</b>	<b>-0.22</b>	<b>254</b>	<b>85</b>	<b>3%</b>	<b>0.197</b>
<b>Cyg X-1</b>	<b>71.33</b>	<b>+3.07</b>	<b>773</b>	<b>1052</b>	<b>79%</b>	<b>0.446</b>
Transient sources			Peak fluxes	Peak fluxes		
<b>1A 0535+262</b>	<b>181.45</b>	<b>-2.64</b>	<b>3813</b>	<b>2819</b>	<b>4%</b>	<b>0.229</b>
<b>GX 304-1</b>	<b>304.10</b>	<b>+1.25</b>	<b>708</b>	<b>347</b>	<b>2%</b>	<b>0.210</b>
<b>GX 339-4</b>	<b>338.94</b>	<b>-4.33</b>	<b>559</b>	<b>792</b>	<b>1%</b>	<b>0.444</b>


Among the transient sources, we take into account only 1A 0535+262, which exhibits quasi-periodic giant outburst that can exceed a peak flux of  $\sim 3$  Crab for a duration of about one month and have a recurrence period ranging between two and four years. We can safely neglect the background increase produced by the two other transient sources in Table 1, GX 304-1 and GX 339-4, which spend only about 1-2% of the time above 500 mCrab flux and have much lower peak fluxes with respect to 1A 0535+262.

After this selection, we end up with eight "candidate contaminant" sources that are expected to increase the LAD background: Crab, Cyg X-1, 1A 0535+262, Vela X-1, GRS 1915+105, 4U 1700-377, Sco X-1 and GX 301-2.

We simulated with Geant4 the contribution of the "contaminant" sources for the fields around specific AGNs, using as input the spectra given by the BAT catalogue. and we found the increments of the LAD background listed in Table 2. For example, we find that the Crab Nebula produces a counting rate ranging from 70 cts/s at  $30^\circ$  off-axis, giving a background increase of  $\sim 3.2\%$ , to  $\sim 13$  cts/s at  $60^\circ$  off-axis, with  $\sim 0.6\%$  increase.

Table 2 - Expected increase in the LAD background from bright and hard point-like persistent sources.

Source			30° off-axis		45° off-axis		60° off-axis	
Name	RA [deg]	dec [deg]	Rate [cts/s]	Increase	Rate [cts/s]	Increase	Rate [cts/s]	Increase
<b>Crab</b>	<b>83.63</b>	<b>+22.01</b>	<b>69</b>	<b>3.2%</b>	<b>42</b>	<b>1.9%</b>	<b>13</b>	<b>0.6%</b>
<b>Vela X-1</b>	<b>135.53</b>	<b>-40.55</b>	<b>2.5</b>	<b>0.1%</b>	<b>2.1</b>	<b>0.09%</b>	<b>0.3</b>	<b>0.01%</b>
<b>GX 301-2</b>	<b>186.66</b>	<b>-62.77</b>	<b>0.7</b>	<b>0.03%</b>	<b>0.3</b>	<b>0.01%</b>	<b>0.1</b>	<b>0.004%</b>
<b>Sco X-1</b>	<b>244.98</b>	<b>-15.64</b>	<b>1.2</b>	<b>0.06%</b>	<b>0.4</b>	<b>0.02%</b>	<b>0.2</b>	<b>0.009%</b>
<b>Cyg X-1</b>	<b>299.59</b>	<b>35.20</b>	<b>68</b>	<b>3.2%</b>	<b>43</b>	<b>2.0%</b>	<b>14</b>	<b>0.7%</b>
<b>GRS 1915+105</b>	<b>288.80</b>	<b>+10.95</b>	<b>6.4</b>	<b>0.3%</b>	<b>3.7</b>	<b>0.2%</b>	<b>1.1</b>	<b>0.05%</b>
<b>4U 1700-377</b>	<b>255.99</b>	<b>-37.84</b>	<b>5.0</b>	<b>0.2%</b>	<b>3.0</b>	<b>0.1%</b>	<b>1.0</b>	<b>0.05%</b>

	<p style="text-align: center;">LOFT</p> <p style="text-align: center;">LAD</p>	<p><b>Doc. no. :</b> LOFT-LAD-BkgSys-20130918  <b>Issue :</b> 1.0  <b>Date :</b> 18 September 2013  <b>Cat :</b>  <b>Page :</b> 12 of 23</p>
---	--	--

The Strong Gravity studies with the LAD are based on the observation of a relatively small number of AGNs (about 35). For these sources we computed the distance from the "candidate contaminants" and we find the following number of AGNs, belonging to this sample, at a distance smaller than  $60^\circ$ :

Source name	Number of AGN "contaminated"
Crab	7
Vela X-1	12
GX 301-2	13
Sco X-1	8
Cyg X-1	3
1A 0535+262	7
GRS 1915+105	8
4U 1700-377	8

Starting on the simulations of the Crab and other sources (see Table 5.2), we can take  $60^\circ$  as the maximum distance at which on average a "contaminant" source can affect the LAD background during the observation of a faint source. With this assumption, we find that only nine AGNs lack any "contaminant" source, while the maximum number of "contaminants" near an AGN is four. The most frequent number of point-like sources at distance  $< 60^\circ$  to any AGN in the sample is two (in fourteen occurrences):

Number of AGNs with 0 sources at distance  $< 60^\circ$ : 9  
Number of AGNs with 1 sources at distance  $< 60^\circ$ : 3  
Number of AGNs with 2 sources at distance  $< 60^\circ$ : 14  
Number of AGNs with 3 sources at distance  $< 60^\circ$ : 5  
Number of AGNs with 4 sources at distance  $< 60^\circ$ : 4  
Number of AGNs with  $\geq 5$  sources at distance  $< 60^\circ$ : 0

As an example, we show in Figure 8 the field around the AGN MRK 509, which has a background increase above 1% produced by "contaminant sources". In the figure, the field is centered on the AGN observed by the LAD and is represented adopting the azimuthal equidistant projection, in which all distances measured from the center of the map (i. e. the target AGN) along any longitudinal line are accurate. The dashed green lines indicate the long and short directions of the field of view of the LOFT WFM, oriented assuming the worst case constraint of an angular distance fixed at  $90^\circ$  between the Sun and the solar panels. The plots are produced for the day when the target AGN at the center of the map is at  $90^\circ$  from the Sun. We can see from the plots that the "candidate contaminant" sources are inside the baseline field of view of the WFM and thus can be efficiently monitored with this instrument.

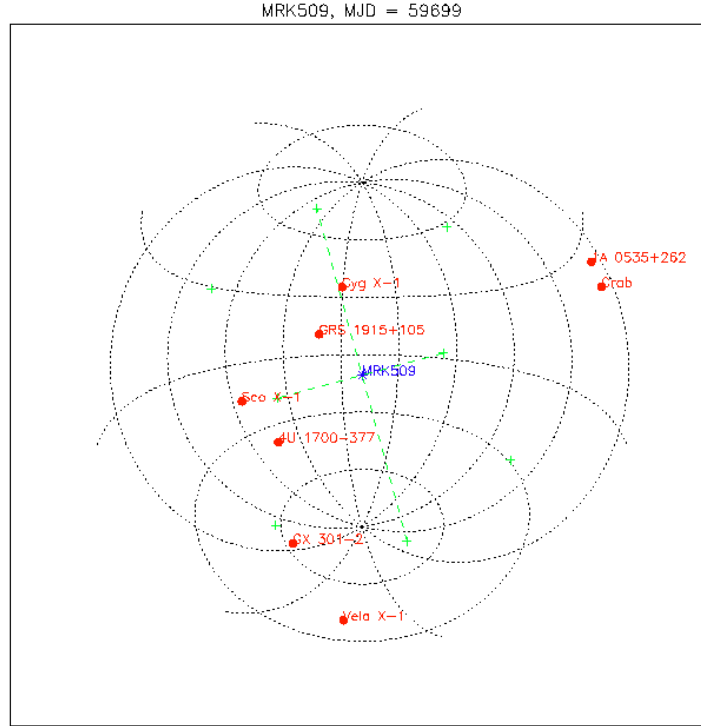


Figure 8 - Field around MRK 509 (blue asterisk) as observed by the LAD. “Contaminant” sources are represented by the red dots. The MJD indicated on top of the figure is the day when the target AGN is at a distance of  $90^\circ$  from the Sun. The orientation of the long direction of the WFM field of view (green dashed lines) follows the worst case constraint of an angular distance fixed at  $90^\circ$  between the Sun and the solar panels. The green crosses indicate the corners of the WFM field of view. In the azimuthal equidistant projection adopted for the map, all distances measured from the center of the map (i. e. the target AGN) along any longitudinal line are accurate but the shape of the WFM field of view is not accurate.

During the observation of MRK 509 the background is expected to increase of  $\sim 2.2\%$ . Almost all the increase ( $\sim 1.8\%$ ) is produced by contribution of Cyg X-1 at  $47^\circ$  distance, with a small contribution from GRS 1915+105 (0.3%) at  $31^\circ$  and 4U 1700-377 (0.07%) at  $56^\circ$ . The spectrum of the increment of the LAD background produced by the “contaminants” is plotted in Figure 9.

It is important to remark here that no target AGN can be simultaneously contaminated by the two brightest point-like sources in Table 2, Crab and Cyg X-1. Conversely, the transient 1A 0535+262 is at just  $4.4^\circ$  from the Crab and, when in outburst, will significantly increase the effect of the Crab itself.

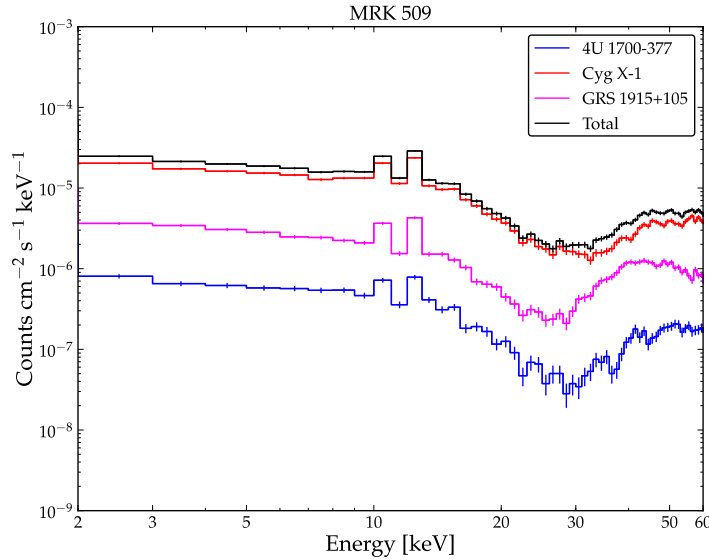


Figure 9 - Simulated spectrum of the increase of the LAD background produced by the “contaminant” sources when observing MRK 509. The simulated increase is  $\sim 47$  cts/s, corresponding to  $\sim 2.2\%$  of the overall background.

Note that since the angle between the boresight and the off-axis contaminating source is constant during the observation, this gives a constant term in the orbital modulation model (Section 3), with the only exception of the (short) times in which the off-axis source is in occultation while the target is not, or viceversa. In other words, for a given target the strong off-axis source contamination affects essentially the absolute background level, and not its modulation.

## 4.2 Solar activity

The X-ray emission from the Sun is continuously monitored by the GOES satellites in two energy bands:  $1-8 \text{ \AA}$  ( $1.5-12 \text{ keV}$ ) and  $0.5-4 \text{ \AA}$  ( $3-25 \text{ keV}$ ). Although extremely intense, ranging from  $10^{-8} \text{ W/m}^2$  (equivalent to  $10^{-5} \text{ erg/cm}^2/\text{s}$ ) to  $5 \times 10^{-6} \text{ W/m}^2$  (corresponding to  $5 \times 10^{-3} \text{ erg/cm}^2/\text{s}$ ), the persistent emission from the Sun is characterised by a steep bremsstrahlung spectrum. The RHESSI upper limit in 3-6 keV during the Sun quiet periods is consistent with a temperature of  $6 \times 10^6 \text{ K}$ , equivalent to 0.5 keV.

We modelled the persistent emission from the Sun with a thermal bremsstrahlung at 0.5 keV energy normalized at  $10^{-5} \text{ erg/cm}^2/\text{s}$  (Solar minimum) and  $5 \times 10^{-3} \text{ erg/cm}^2/\text{s}$  (Solar maximum) in the 1.5-12 keV band. Preliminary simulations of the Sun persistent emission in this *maximum* conditions give an overall efficiency of  $\sim 2 \times 10^{-9}$  for the LAD at  $60^\circ$ . This can be considered as a worst case since the requirement for the angular distance from the Sun and the pointing axis is  $90^\circ \pm 30^\circ$ . These simulations indicate a small contribution,  $\sim 200 \text{ cts/s}$  (equivalent to  $\sim 5\%$  of the overall rate), for the LAD from the Sun in this worst case. Again, this is a constant contribution (the variability is on long timescales) to the orbital modulation of the background during the observation of a given target.

Major Solar flares are bright at hard X-rays and are detected up to gamma-rays. For example, solar flares are detected by the SuperAGILE hard X-monitor of the AGILE

	<p style="text-align: center;">LOFT</p> <p style="text-align: center;">LAD</p>	<p><b>Doc. no. :</b> LOFT-LAD-BkgSys-20130918  <b>Issue :</b> 1.0  <b>Date :</b> 18 September 2013  <b>Cat :</b>  <b>Page :</b> 15 of 23</p>
---	--	--

mission above 20 keV through the collimator shielding. In this case the angle between the AGILE pointing axis and the Sun is fixed at 90°.

Dennis et al. (2005) describe the analysis of an M2 class solar flare (26 April 2003) observed by RHESSI (3-20 keV) and RESIK (2.0-3.7 keV). Their model is a thermal bremsstrahlung with a temperature of  $18.6 \times 10^6$  K. M2 class is equivalent to a peak flux of  $2 \times 10^{-5}$  W/m<sup>2</sup> (that is  $2 \times 10^{-2}$  erg/cm<sup>2</sup>/s) in the GOES 1.5 – 12 keV band, thus giving a non-negligible contribution to the LAD background. In any case, solar flares are transient events (from a few seconds to an hour), easily recognized, allowing to filter out from an observation the times of a flare occurrence.

### 4.3 The Galactic Ridge X-ray Emission (GRXE)

A diffuse X-ray emission is observed from the Galactic Plane, historically known as the Galactic Ridge X-ray Emission (GRXE), and is explained as the superposition of the emission from faint and unresolved sources (see e. g. [RD6, RD7]). A wide-energy spectrum of the GRXE accumulated in the 3-400 keV energy band from observations of the "Scutum Arm" ( $l = 33^\circ$ ,  $b=0^\circ$ ) with RXTE/PCA and CGRO/OSSE is reported by [RD8], although CGRO/OSSE data are probably contaminated by discrete sources [RD7]. Neglecting the higher energy region of the spectrum, the low-energy one (3–20 keV from RXTE/PCA) can be approximated by a power law of photon index  $\sim 2.1$ .

At higher energies, of more interest to study the component that may leak through the LAD collimator, the GRXE has been observed by INTEGRAL/IBIS in 17–60 keV [RD6]. After the subtraction of the discrete point-like sources, the diffuse emission extends in a region of  $100^\circ \times 5^\circ$  and peaks at  $\sim 150$  mCrab (roughly equivalent to  $\sim 1.5 \times 10^{-9}$  erg/cm<sup>2</sup>/s in 17–60 keV) at the Galactic Center. Moreover, the diffuse emission is found to be spatially correlated with the NIR map of the Galaxy from the COBE/DIRBE data at 4.9  $\mu$ m. Given the soft spectrum of the GRXE, we do not expect it to be an important contribution to the instrumental background.

## 5 Blank field monitoring

The geometrical model described in Section 3 has to be properly calibrated using in-orbit flat fields. That is, the analytical parameters that describe the shape of the background modulation as a function of the angle  $\theta_E$  have to be verified by fitting the observed background modulation when pointing to "blank" fields, i.e. sky regions at different celestial declinations without significant sources.

This is anticipated to allow for a background prediction at a level significantly better than 1% in the 2–10 keV band, which is the LAD science requirement. Such a level of systematic uncertainty was indeed already reached by the past experiment RXTE/PCA, which, in the presence of a much more variable background level (250% vs 8%) and less predictable background sources, with an appropriate modeling reached the level of  $\sim 1\%$  [RD2, RD3, RD4].

In the following three figures, the background modulation factor (i.e. the instantaneous background flux in the 2-30 keV band with respect to its orbital average) is shown for a blank field pointing at a declination of 30°, along five consecutive orbits (5 orbits of 90 minutes correspond to  $\sim 27$  ks). The gray points indicate the observed flux accumulated in 5 min (300 s) integrations, while the red curve is the modelled flux and the blue curve is the model resulting from a fit of the observed values. The fit residuals show that the



systematics level of the background reconstruction is lower than 0.1%.

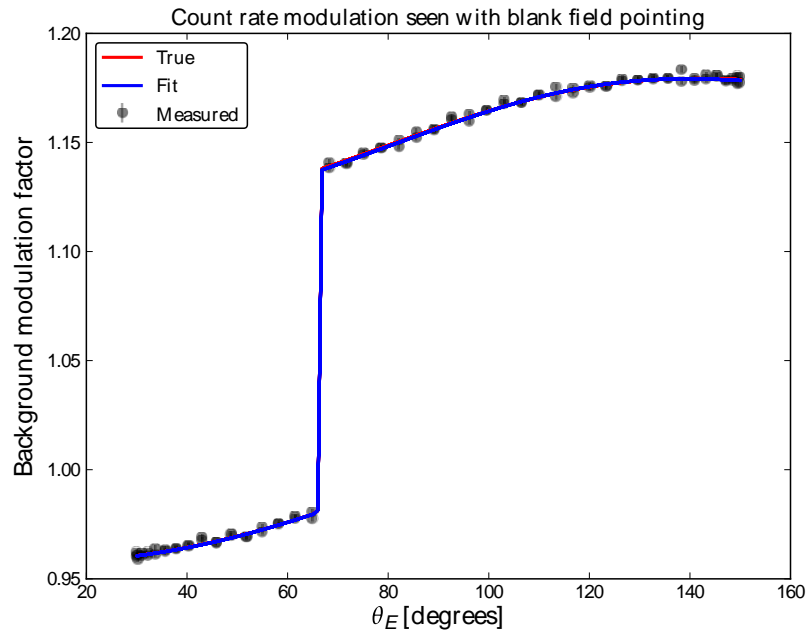


Figure 10 - Simulation of the background modulation factor as a function of  $\theta_E$ . The large jump is due to the Earth occultation.

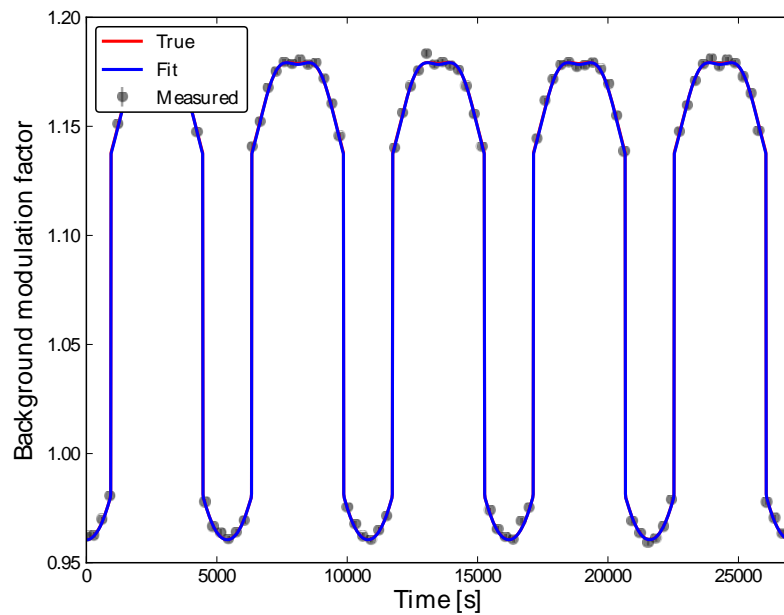


Figure 11 - Background as a function of the time. Five orbits are shown.

	<p>LOFT</p> <p>LAD</p>	<p><b>Doc. no. :</b> LOFT-LAD-BkgSys-20130918</p> <p><b>Issue :</b> 1.0</p> <p><b>Date :</b> 18 September 2013</p> <p><b>Cat :</b></p> <p><b>Page :</b> 17 of 23</p>
---	------------------------	--

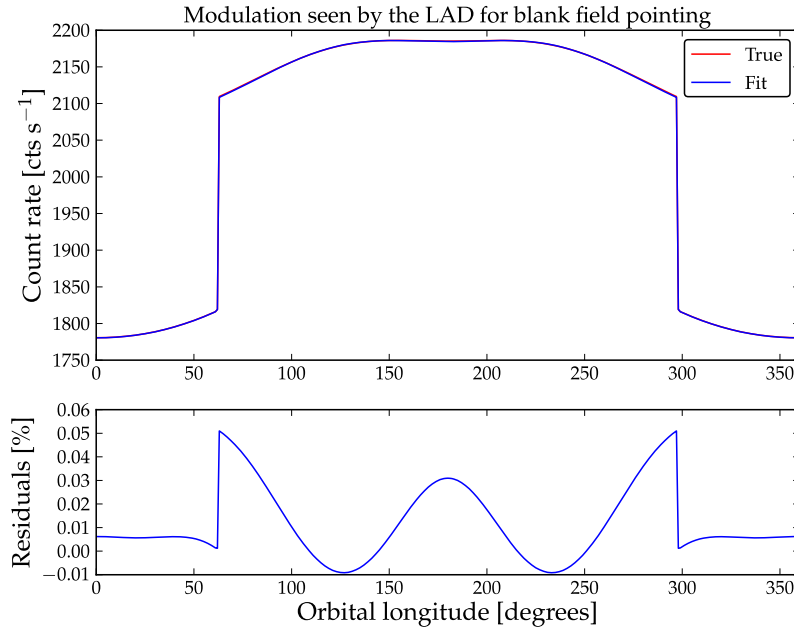


Figure 12 - Residuals of the model fitting for the orbital modulation of the background.

## 6 Active monitoring

However, as some of the LOFT science cases (in particular the extragalactic science) will benefit from reaching a background knowledge significantly better than the requirement, an *active* background monitoring was designed for the LAD, to further improve the modeling. Due to the slow and smooth background variation, there is no need for a high-statistics, instantaneous monitoring of the rate: rather, a continuous *benchmark* of the slow modulation will allow for a real-time verification of the background model. This active background monitoring is achieved by the introduction of a “blocked collimator” (a collimator with the same stopping power but no holes) for an area corresponding to one Module of the LAD,  $\sim 1200 \text{ cm}^2$ , composed of 16 SDDs.

The blocked collimator will enable the continuous monitor of all components of the LAD background, with the exception of the aperture background, accounting for  $\sim 90 \%$  of the total background, and also evaluating the long-term variations (e.g. linked to the Solar cycle, see Section 4.2) and fast ( $\sim \text{min}$  timescale) flaring transients.

Figure 13 shows the count rate measured by the blocked module in 300 s integrations, along 10 orbits ( $\sim 55 \text{ ks}$ ) in which the LAD boresight is at  $\delta = 30^\circ$ . In this case, the accuracy for reconstruction of the background modulation reaches typical levels of about 0.1%-0.3%.



# LOFT LAD

**Doc. no. :** LOFT-LAD-BkgSys-20130918  
**Issue :** 1.0  
**Date :** 18 September 2013  
**Cat :**  
**Page :** 18 of 23

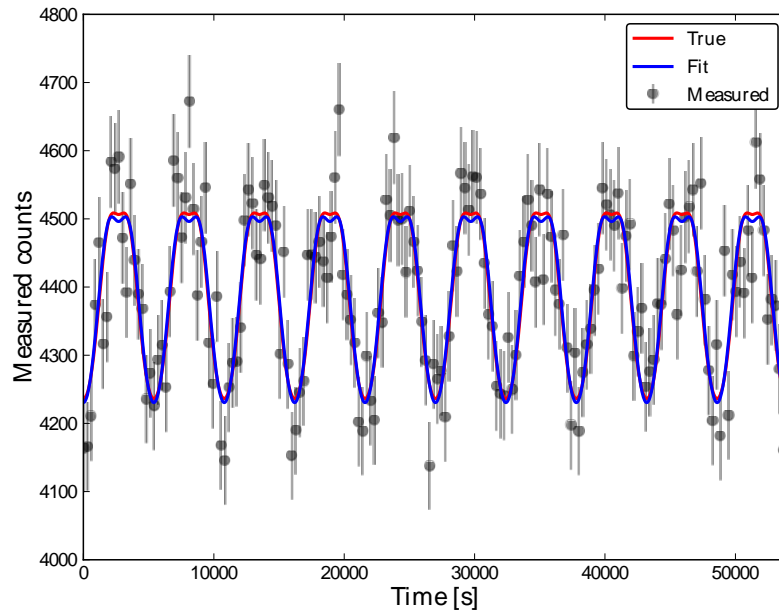


Figure 13 - Count rate observed by the blocked module, for a 10 orbit observation pointing at a declination of  $30^\circ$ .


## 7 Conclusions

Under the assumption of a steady photon background (CXB plus Earth albedo), the orbital modulation of the LAD background is very well described by a phenomenological model (gaussians at fixed boresight-to-Earth angle). The amplitude of the modulation along the orbit depends on the angle between the pointing direction and the Earth.

Blank field observations at different latitudes will provide experimental data for the background model, allowing its calibration. The model will thus be valid for any source location. Once the model is calibrated at the start of the mission, periodic short blank field observations will provide benchmark/updates to the model.

Preliminary simulation results show anticipated accuracies of  $\sim 0.1\%$ .

For the active monitoring, it should be considered that most of the LAD background is "dependent on mass" (the aperture background is a fraction of only 13%), and that the background variation is a smooth orbital modulation (i.e., no instantaneous or short-timescale variations are expected). Therefore, there is no requirement for a real-time monitoring of the background with the same area as the signal: the shape of the background modulation is constrained. Monitoring the background with one module out of 126 (i.e. 16 detectors out of 2016) will provide enough statistics to continuously benchmark the background modulation curve, already modeled by the geometrical model. A "closed" collimator with the same "effective mass" (identical material and mass but no holes) will monitor all background components (87%) except for the aperture. The cost in terms of effective area is just 0.8%. Moreover, the active monitoring will work all the time, in any attitude, providing a library of background rates for the whole

	<p>LOFT</p> <p>LAD</p>	<p><b>Doc. no. :</b> LOFT-LAD-BkgSys-20130918  <b>Issue :</b> 1.0  <b>Date :</b> 18 September 2013  <b>Cat :</b>  <b>Page :</b> 19 of 23</p>
---	------------------------	--

duration of the mission.

Within the limits of its relatively small collecting area, the closed module" will detect any background rate increase due to unexpected and unpredictable events (e.g., solar flares, particle events, ...) enabling correction and/or selection of data. Using the "closed module" only (i.e. assuming no information from the blank fields), simulations show preliminary anticipated accuracies of <0.5%.

The contribution of strong offaxis "contaminant" sources is usually inside the baseline field of view of the WFM and thus can be efficiently monitored with this instrument.

	<p style="text-align: center;">LOFT</p> <p style="text-align: center;">LAD</p>	<p><b>Doc. no. :</b> LOFT-LAD-BkgSys-20130918  <b>Issue :</b> 1.0  <b>Date :</b> 18 September 2013  <b>Cat :</b>  <b>Page :</b> 20 of 23</p>
---	--	--

## 8 Appendix 1 - Context: The RXTE/PCA background modelling

The Proportional Counter Array (PCA) aboard RXTE was a large area proportional counter composed of five independent units (each consisting of a propane veto layer, followed by three Xenon gas layers) with an overall collecting area of 6500 cm<sup>2</sup> and a collimator with ~1° field of view. RXTE had an orbit with 580 km altitude and 23° inclination. It is important to note that the altitude varied by 20 km per spacecraft orbit, and that the altitude steadily decreased over the lifetime of the mission. Furthermore, there were long-term orbital trends such as precession of the orbital plane on ~52 day time scales, as well as precession of perigee on a similar time scale.

PCA was a non-imaging instrument, although slew scans were used to map and monitor the Galactic bulge region. For both spectroscopy and timing studies, the background was subtracted based on a time-dependent empirical model, developed from repeated observations of both “blank sky” regions as well as dark Earth observations. The background was defined as the contribution of “non-source” counts that were composed of the local particle environment, the activation of the spacecraft materials due to the passages through the SAA, and the CXB. Contributions from Galactic ridge emission [RD7] were not part of any background model, even though such backgrounds were relevant for observations of faint Galactic objects, nor were included counts from nearby sources within the field of view of the collimator. For the former case, typically users would either include a spectral model component for the Galactic ridge emission (e.g., thermal Bremsstrahlung), or would use a suitable “ridge only” PCA observation as an additional background file. (Such methods were predominantly for spectral studies; Galactic ridge emission was usually not expected to affect timing observations beyond expectations of Poisson statistics.)

Interference by nearby contaminating sources (which was likely to be relevant for both spectral and timing studies) was a potential issue for a number of well-studied objects, e.g., NGC 5548 and most Galactic center/bulge sources. Such situations were typically dealt with by performing offset pointings of the source of interest in directions away from the interfering source. A 30 arcminute offset would eliminate nearly entirely any source > 0.5°, while reducing the effective area for the source of interest by approximately one half.


Similar procedures will likely be required for 15%-20% of LOFT sources, as described in the technical note by Wilms et al., [LOFT\\_LAD\\_SrcConf\\_20120402](#).

The background estimate that was provided for the PCA in general varied as a function of time and location within the PCA orbit. The magnitude of the fluctuations with time, as well as the expected variance of the CDXB, set the limit below which the flux of sources cannot be determined at  $4 \times 10^{-12}$  erg/cm<sup>2</sup>/s in the 2-10 keV band, which corresponds to 0.2 mCrab.

The method used to calibrate the background of PCA is described by [RD2] and is based on the following empirical model, defined for each energy channel  $i$ :

$$BKG_i = A_i + B_i \times (L7 \text{ or } VLE) + C_i \times DOSE + D_i \times (t - t_0)$$

$A_i$  is a term that accounts for the field-to-field variation of the CDXB in the 1° field of view (Revnivtsev et al., 2003);  $B_i \times (L7 \text{ or } VLE)$  contains the variation of the background counting rate along the satellite orbit, measured either with the “L7” anti-coincidence rate (suitable for faint sources, approximately < 50 mCrab), or the “Very Large Event” (VLE) rate (suitable for not too bright sources; very bright sources ~> 500 mCrab have a VLE rate dependent upon source rate);  $C_i \times DOSE$  is the contribution of the activation of the instrument and spacecraft material and depends on the counting rate of the

	<p style="text-align: center;">LOFT</p> <p style="text-align: center;">LAD</p>	<p><b>Doc. no. :</b> LOFT-LAD-BkgSys-20130918</p> <p><b>Issue :</b> 1.0</p> <p><b>Date :</b> 18 September 2013</p> <p><b>Cat :</b></p> <p><b>Page :</b> 21 of 23</p>
---	--	--

HEXTE particle monitor (DOSE) inside the SAA, with a portion of the activation decaying on a 24 minute time scale and another component decaying on a 240 minute time scale;  $D_i \times (t - t_0)$  is a “secular” term that takes into account the variation of the satellite altitude with time.

All of the above coefficients were time dependent. Time dependence was introduced by multiple factors. The detector gain varied with time, and there were several discrete instances of changing the high energy voltage of the PCA detectors. (These discrete changes are referred to as “Epochs”, of which there were 5 major ones. Secular drifts in gain occurred throughout all Epochs, but large, discontinuous changes were imposed at the start of each new Epoch.) The spacecraft orbit decayed with time — altering the particle and activation backgrounds — but additionally, the atmosphere rose during periods of solar maximum, which provided more shielding against particle background, albeit during periods when the background was on average higher. The satellite orbit precessed on 52 day time scales. Thus, it was deemed important to measure the spacecraft background over time scales significantly shorter than all of these known and suspected time scales.


In practice, the parameters  $A_i$ ,  $B_i$ ,  $C_i$  and  $D_i$  were obtained by fitting a series of six blank field sky observations that occurred twice a day. The twice daily time scale was chosen to be significantly shorter than the known evolution time scales of the spacecraft orbit, and to coincide with the time scale of a series of precisely twice daily AGN monitoring observations that were designed to determine X-ray power spectra of those objects. The exposure time for each of the six blank Sky fields were 1600 s. This exposure time was considered the shortest integration time over which one could reliably obtain a background estimate for the faintest PCA observations.

The twice daily cadence of these background observations began in 1999 (slightly more than three years after launch), which is near the time that RXTE began frequent AGN monitoring, and continued without minimal interruption throughout the remainder of the mission. RXTE was a very rapidly slewing spacecraft, meaning that multiple short observations was significantly less of a burden on observational efficiency than it would have been for many other missions.


The background variance obtained with these methods ranged between 2% (at 2-10 keV) to 1% (at 10-20 keV), and represents an uncertainty of the overall background normalization over these energy bands (each containing a few dozen spectral channels). Users studying spectra of sources where background subtraction is important often allow the scaling of the absolute normalization of the background to become a fit parameter that is free to vary fractionally from unity by 1–2% (i.e., the XSPEC “corfile” procedure). This procedure is often found to usefully improve spectral fits to faint sources, although no formal study has been conducted to determine the level of residual variance after performing this procedure.

It is also important to note that the PCA background estimation procedures were not fully anticipated prior to launch of the spacecraft. The “L7” anti-coincidence rate and VLE rate as monitors of the particle background, and especially the use of the HEXTE particle monitor to measure the activation background, were developed after launch of the mission. For purposes of observing the spectra of AGN, development of this model to a sufficient degree of fidelity for use on such faint sources required several years.

We expect for LOFT a smaller modulation of the background and a less important contribution of the activation of the spacecraft materials, thanks to the baseline orbit at the inclination of  $<5^\circ$ . On the other hand, the LAD collimator is more transparent than the PCA one and we expect a higher background component leaking through the collimator (see Section 2). Both CXB and Galactic Ridge emission will be sources of

	<p>LOFT</p> <p>LAD</p>	<p><b>Doc. no. :</b> LOFT-LAD-BkgSys-20130918  <b>Issue :</b> 1.0  <b>Date :</b> 18 September 2013  <b>Cat :</b>  <b>Page :</b> 22 of 23</p>
---	------------------------	--

background for LOFT as well; however, all sky surveys by, e.g., eRosita [RD9], may allow for more detailed accounting of these components than was possible for PCA.

	<p>LOFT</p> <p>LAD</p>	<p><b>Doc. no.</b> : LOFT-LAD-BkgSys-20130918</p> <p><b>Issue</b> : 1.0</p> <p><b>Date</b> : 18 September 2013</p> <p><b>Cat</b> :</p> <p><b>Page</b> : 23 of 23</p>
---	------------------------	--

## 9 References

- [RD1] Campana et al. (2013), *Exp. Astr.*, in press.
- [RD2] Jahoda et al. (2006), *ApJSS*, **163**, 401.
- [RD3] Shaposhnikov et al. (2012), *ApJ*, **757**, 159.
- [RD4] Cusumano et al. (2010), *A&A*, **524**, A64.
- [RD5] Dennis et al. (2005), *Adv. Sp. Res.*, **35**, 1723.
- [RD6] Krivonos et al. (2007), *A&A*, **463**, 957.
- [RD7] Revnivitsev et al. (2006), *A&A*, **452**, 169.
- [RD8] Valinia et al. (2000), *ApJ*, **534**, 277.
- [RD9] Merloni et al. (2012), *arXiv:1209.3114v2*.